ADVANCED SUSTAINABLE SYSTEMS
www.advsustainsys.com

Electronic Waste to Energy: Self-Powered Electronic Devices and Organic Dye Degradation Using TENG-Assisted Photocatalysis

Anusha Kaki, Gouranga Maharana, Navaneeth Madathil, Velupula Mahesh, Khanapuram Uday Kumar, Paul Joseph Daniel, and Rakesh Kumar Rajaboina**

Electronic waste (e-waste) and the use of portable electronic devices are rapidly increasing due to technological advancements globally, leading to harmful effects on the environment. E-waste causes severe environmental damage, such as the pollution of soil, water, and air. Therefore, there is an urge for effective e-waste management, recycling, and sustainable consumption. In this report, We developed high-performance triboelectric nanogenerators (TENGs) utilizing discarded laptop LCD screens as triboelectric layers for energy harvesting and organic dye pollutant degradation. Among all the fabricated devices, the LCDW4-TENG exhibited exceptional performance with fluorinated ethylene propylene (FEP) as the opposite frictional layer, yielding a V_{oc} of ≈470 V, I_{sc} of ≈ 143 μA, and a power density of 5.04 W m^{-2} at a load resistance of 1 MΩ. The long-term stability of the device is tested over 6,000 cycles and is found to be very stable. This e-waste-based TENG is employed in the treatment of methylene blue organic dye through TENG-assisted photocatalysis. An enhanced degradation efficiency of methylene blue dye is observed with the support of TENG. This work highlights the potential of LCD waste-derived TENGs for driving self-powered electronic devices and environmental remediation applications thereby contributing to the circular economy concept.

1. Introduction

Electronic waste (e-waste) accumulation has rapidly increased due to technological advancements, population growth, and shortcomings in waste management practices, leading to serious environmental challenges.[1–4] The primary sources of waste include plastics, discarded electronic gadgets, household, medical, textile, and discarded automotive parts. To tackle the environmental problems caused by waste, various utilization strategies—such as recycling, upcycling, and reuse — are implemented. Another impressive strategy is waste-to-energy (WTE) conversion, which has gained widespread adoption.[3,5–12] These approaches are crucial for mitigating environmental degradation and promoting a greener planet. The WTE technologies have garnered significant attention due to their potential to generate electrical energy and other energy resources, positioning them as a promising solution for achieving a green and sustainable future.[7,9,10] The WTE methods primarily consist of incineration, biogas production, pyrolysis, gasification, and waste-derived fuels. However, many of these technologies have inherent drawbacks, including the release of harmful emissions, high initial and operational costs, and the generation of toxic residues and byproducts. To address these challenges, there is an urgent need to develop next-generation WTE technologies that effectively utilize waste while minimizing environmental harm. In this context, Triboelectric Nanogenerators (TENGs) have emerged as a promising alternative for sustainable energy generation.[13–15] TENG technology enables the reuse of waste materials to generate clean and renewable electrical energy, providing an eco-friendly and efficient approach to waste-to-energy conversion.

In 2012, Prof. Z. L. Wang introduced the first triboelectric generator (TENG) for mechanical energy harvesting, based on the principles of contact electrification and electrostatic induction.[16] In the following years, extensive research focused on establishing theoretical foundations,[17–19] exploring various operating modes,[20,21] optimizing material choices,[22–25] designing innovative structures,[26] and developing advanced energy management circuits for TENG technology.[27] Among the four operating modes of TENG, the vertical contact-separation (VCS) mode is the most commonly used. In this mode, two materials with different triboelectric properties come into contact and separate repeatedly, inducing an alternating current (AC) in the external circuit. The triboelectric layers in TENGs can be composed of polymers, metal oxides, 2D materials, metals, and porous materials, with each offering unique advantages for energy conversion,[22,28–31]

A. Kaki, G. Maharana, N. Madathil, V. Mahesh, K. U. Kumar, P. J. Daniel, R. K. Rajaboina
Department of Physics
Energy Materials and Devices (EMD) Lab
National Institute of Technology
Warangal 506004, India
E-mail: paul@nitw.ac.in; rakeshr@nitw.ac.in

The ORCID identification number(s) for the author(s) of this article can be found under https://doi.org/10.1002/adsu.202500235

DOI: 10.1002/adsu.202500235

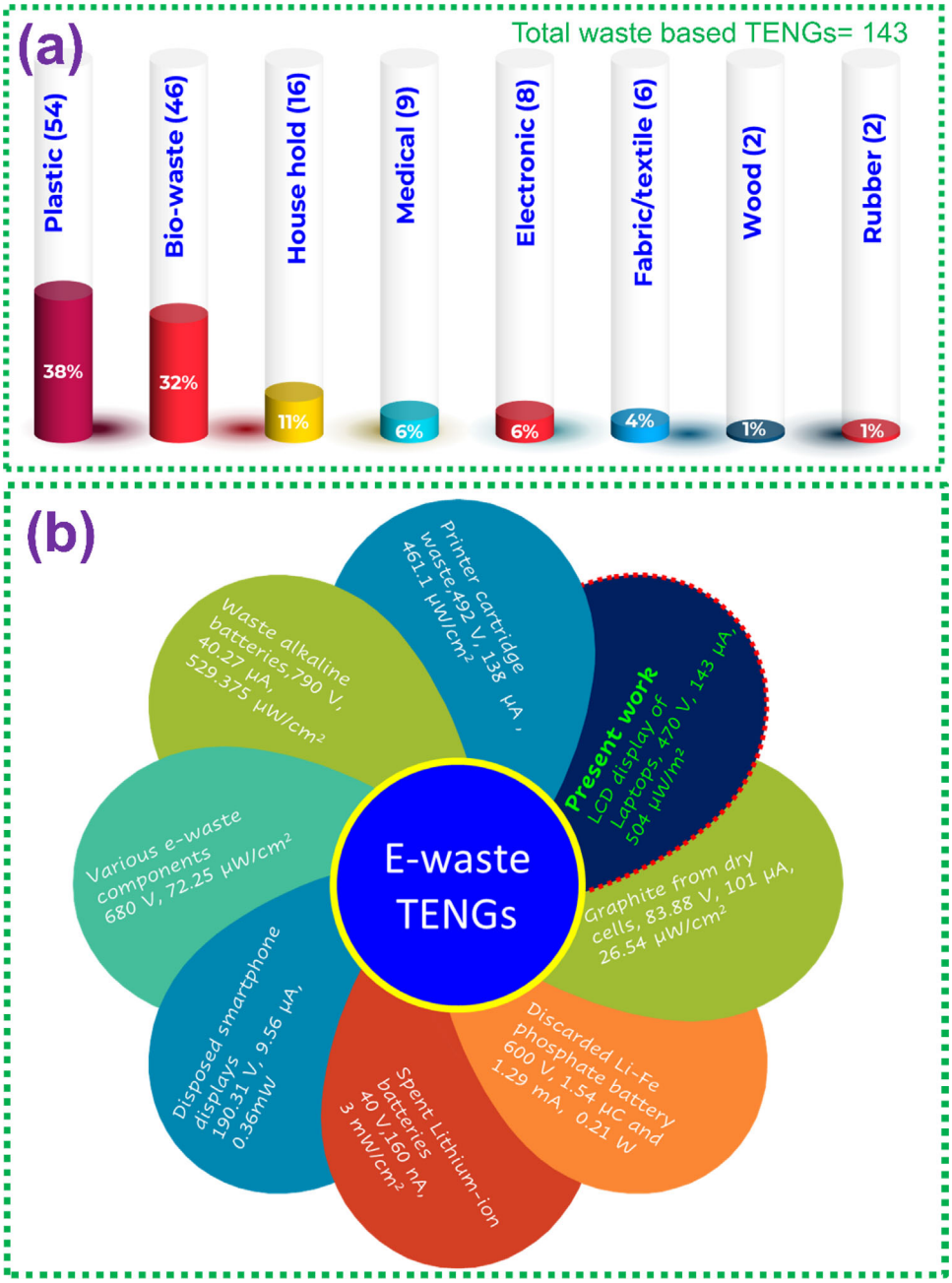

Figure 1. a) Statistical review of several waste-based TENGs and counts indicate the number of publications for each type of waste, b) Literature review of different electronic waste-based TENGs, and their electrical output performance.

By 2018, researchers began exploring the use of waste materials in TENG device fabrication, marking a significant shift toward sustainable energy harvesting.[32] Since then, the application of waste-derived materials in TENGs has grown exponentially, as illustrated in **Figure** 1a.[13–15] There are around 143 publications based on waste-based TENGs. Figure 1a shows the number of publications with different types of waste materials utilized in TENG devices. The data was generated from the Web of Science with keywords triboelectric nanogenerators and waste materials. It is clear that e-waste is one of the least explored areas in TENG design. A detailed review of e-waste-based TENGs and their performance is presented in Figure 1b.[33–39] In the present manuscript, electronic waste, namely laptop LCD display waste is explored for TENG devices and demonstrated for utilization in various applications.

Electronic waste encompasses a wide range of discarded electrical and electronic devices, including household and office appliances as well as personal gadgets. Commonly discarded items in electronic waste includes refrigerators, washing machines, microwaves, televisions, digital cameras, speakers, mobile phones, laptops, tablets, printers, networking equipment, fax machines, photocopiers, batteries, power storage devices, and chargers.

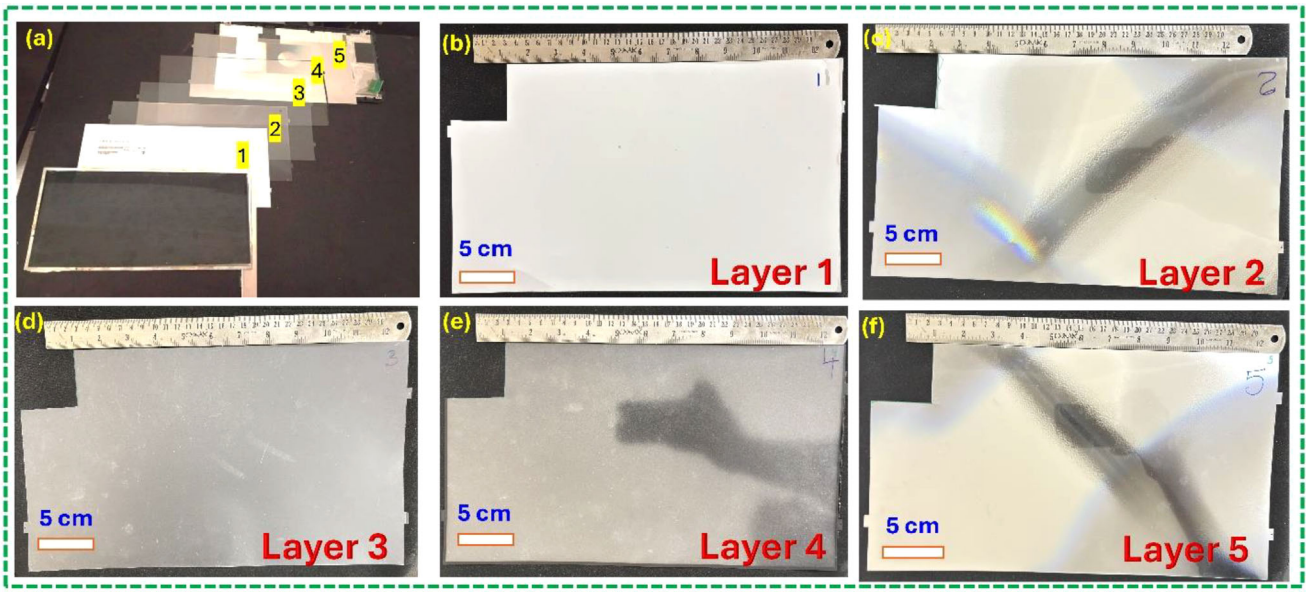

Figure 2. a) Photograph of the LCD screen assembly, b–f) Photographs of the individual layers (1 to 5).

Researchers have already explored a few of the e-wastes in the design of TENGs, as detailed in Figure 1b. Discarded LCD displays of the laptop are not explored and tested as of now. There are several reasons for LCD e-waste generation a) manufacturers often design devices with integrated screens that are difficult or expensive to repair, encouraging users to replace the entire device rather than just the screen, b) rapid technological advancements such as newer displays technologies like OLED, AMOLED, and mini-LED and short product lifecycles, c) high consumer demand for better resolution, slimmer designs, and enhanced features, significantly contributes to LCD e-waste generation within a short span of time. LCD screen wastes mainly produces thin flexible sheets such as polarizing filter layers, color filter layers, ITO-coated layers, liquid crystal, etc. These layers being flat and in rectangular shape with larger area are effectively utilized in the TENG design in the present work.

TENGs have been explored as both sensing elements and power sources in various self-powered applications.[40–42] They enable gas, pressure, touch, force, and chemical sensing.[43,44] Furthermore, TENGs have also been utilized to power portable electronic devices and LEDs without relying on external power.[44] As a power source, TENGs facilitate electrodeposition, electroplating, photo/electrocatalysis, hydrogen production, electrospinning, and ozone generation, showcasing their potential for sustainable and autonomous technologies.[19] However, the use of TENGs in environmental treatment systems, particularly for

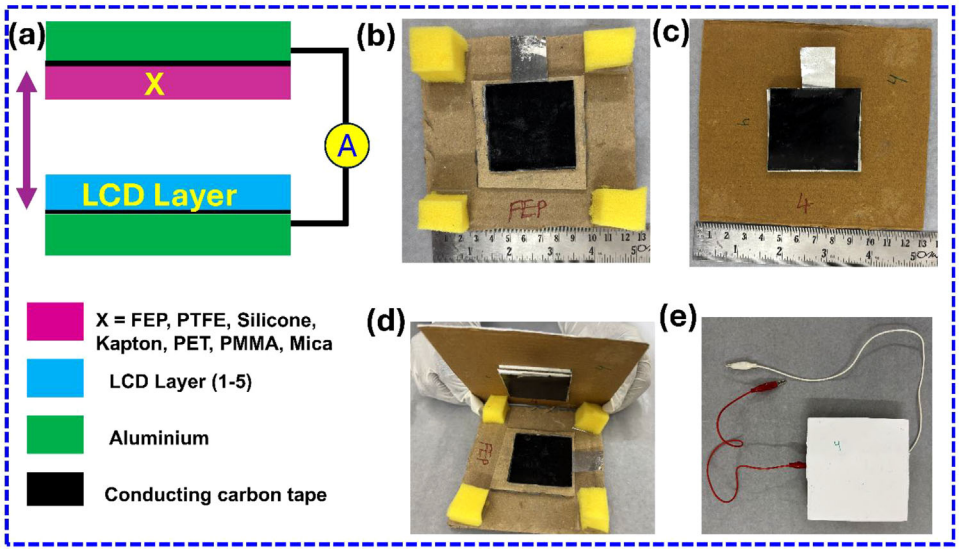

Figure 3. a) Schematics of the TENG device and its frictional layers, b–d) LCD TENG device fabrication steps with the completed real-time photograph of the device (e) Final TENG device with electrical leads from bottom and top electrodes.

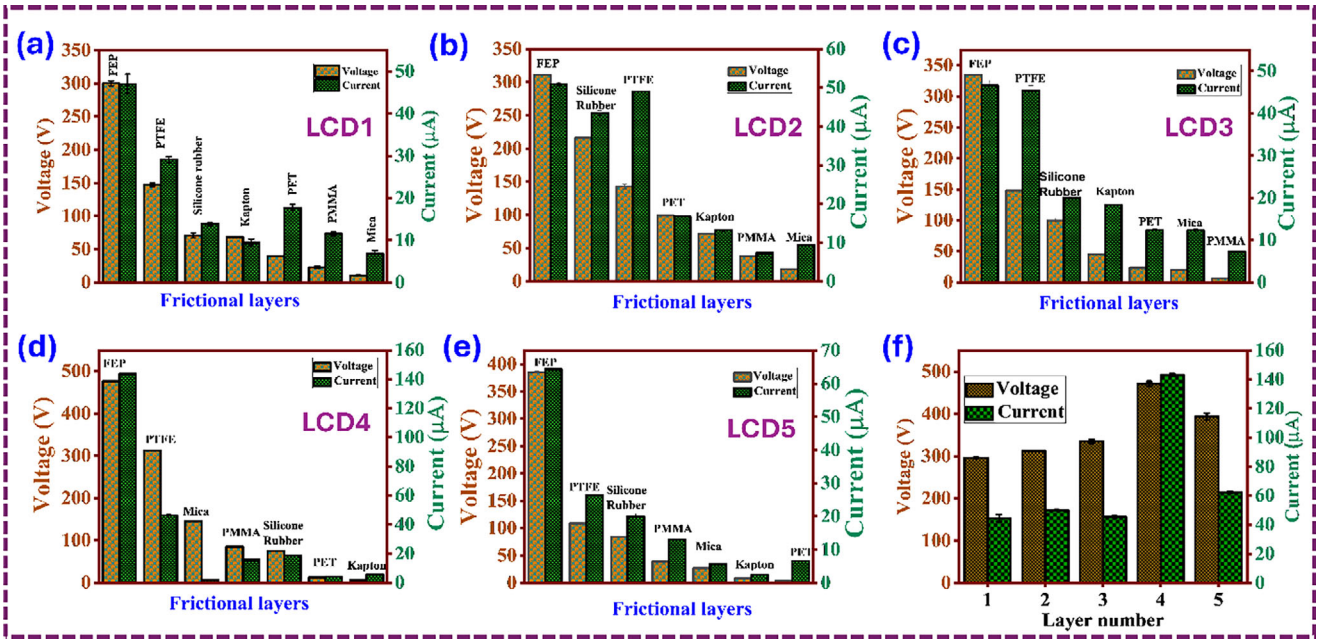

Figure 4. a–e) Electrical output of each LCD layer-based TENG devices with different opposite frictional layers (f) comparison of the best output values of all the fabricated LCD TENG devices.

wastewater purification and organic pollutant degradation, remains limited, as evidenced by the relatively few numbers of research papers available.[45–52] In this manuscript, LCD waste-based TENG device is demonstrated by utilizing it to degrade the methylene blue dye (MB dye) pollutant.

Organic pollutant degradation is essential for maintaining environmental sustainability, safeguarding human health, and ensuring access to clean water resources.[53–55] Industrialization, urbanization, and the excessive use of synthetic chemicals have led to the accumulation of hazardous pollutants, including heavy metals, dyes, pharmaceuticals, pesticides, and organic waste, in water bodies. These pollutants pose significant environmental and health risks, as many are toxic, non-biodegradable, and capable of bioaccumulating in the food chain of living organisms. Effective degradation and removal of these pollutants are crucial for mitigating these risks and ensuring safe water for consumption, agriculture, and industrial use. Traditional methods for pollutant degradation, such as chemical oxidation, biological treatment, and physical separation, have long been used for wastewater purification. Recently, TENG-assisted pollutant degradation has been introduced to enhance degradation efficiency.[46,56] In TENG-assisted degradation, TENG DC output is utilized to drive electrochemical and photocatalytic degradation.[47,57] This approach reduces reliance on external power sources while providing an eco-friendly WTE solution for organic pollutant removal. The present manuscript builds on these advancements by

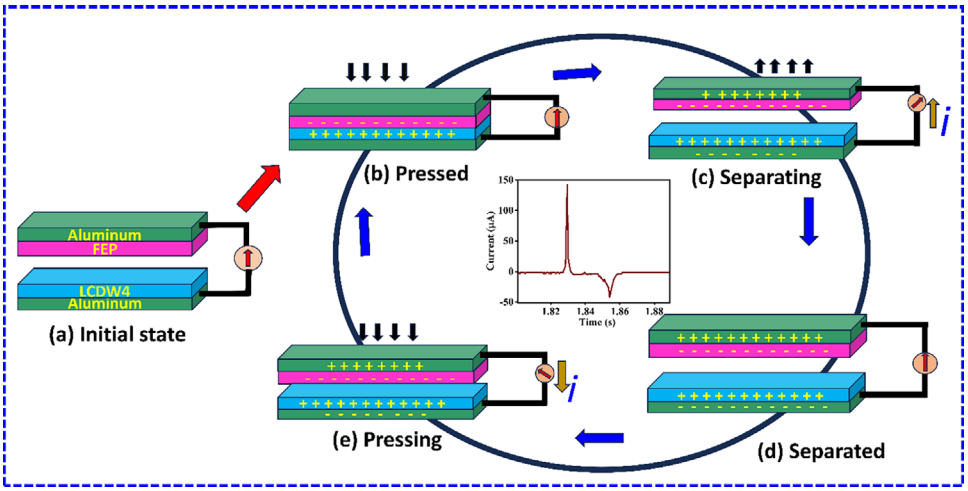

Figure 5. Schematics of the working mechanism of LCDW4-FEP TENG device.

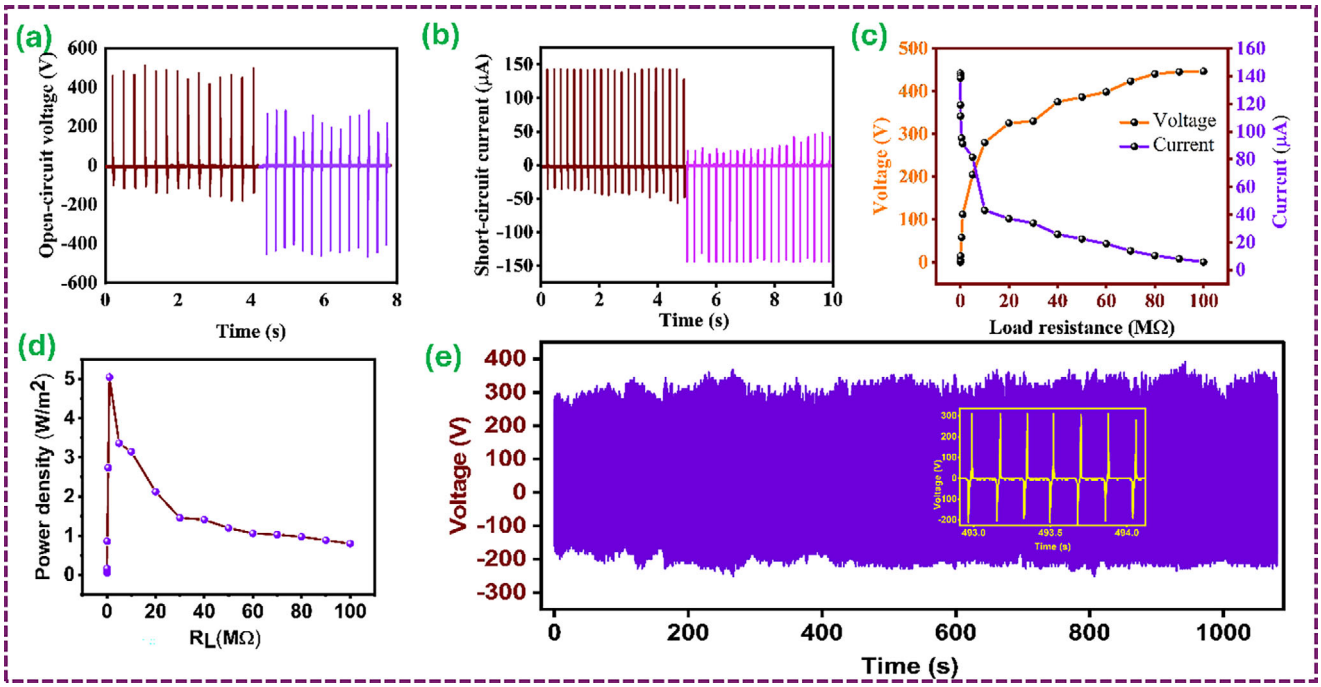

Figure 6. LCDW4-FEP TENG device characteristics: switching polarity test results a) open-circuit voltage, b) short-circuit current, c) load characteristics of TENG, d) instantaneous power density, e) stability of the device tested over ≈6000 cycles (inset: magnified view of few cycles).

upcycling e-waste LCD screens to fabricate a TENG-based system for the self-powered degradation of organic MB dye pollutant. This approach not only promotes clean energy harvesting but also aligns with the circular economy concept by repurposing electronic waste for environmental remediation.

In this manuscript, LCD screen waste is utilized in the TENG design without major modifications, achieving a power density of 5.04 W m^{-2}. A detailed investigation was performed to confirm the optimal triboelectric pair using LCD waste. Furthermore, the LCD waste-based TENG is employed to power LEDs and portable electronic devices and is also demonstrated for use in environmental remediation.

2. Experimental Section

2.1. Materials

Discarded non-functional laptop LCD screens were collected from local service shops in Hanmakonda, Telangana, India. A photograph of the collected LCD is shown in Figure S1 (Supporting Information). Inside the LCD screen, there are five sheets (layers) that support its operation, as illustrated in **Figure** 2a–f. These layers are cut into 5 × 5 cm^2 and used as a frictional layer in the TENG design. Double-sided carbon tape was purchased from Agar Scientific (UK), while cardboard, aluminum sheet electrodes, and sponge spacers were acquired from the local market. To demonstrate the organic dye degradation using the fabricated TENG devices, methylene blue is taken as the standard test dye and the glassy carbon plates (Length 2 cm × Breadth 1.5 cm × Thickness 0.3 cm) were used as the electrodes delivering the TENG DC output power to the dye solution.

2.2. Fabrication of TENG

Figure 3a presents a schematic of the TENG device, where one frictional layer is an LCD layer and the opposite one is chosen from well-known triboelectric materials such as FEP, PTFE, silicone, Kapton, PET, PMMA, and mica. Each LCD layer pairs with different opposite frictional layers to determine the best triboelectric combination. The most efficient pair will be selected for detailed characterization and application studies. Figure 3b–d shows photographs of the frictional layers and the fabricated TENG device using an LCD layer and FEP as the triboelectric pair. The fabrication process starts by attaching the selected LCD layer to an aluminum substrate with conductive carbon tape and securing it onto a pre-defined cardboard base (Figure 3c). Likewise, the FEP sheet is affixed to another pre-defined cardboard base (Figure 3b), with four sponge spacers placed in the corners to create a finite gap between the frictional layers after the assembly. Next, the FEP layer cardboard is positioned over the LCD layer cardboard, and spacers are secured with double-sided tape at all the four corners, as shown in Figure 3d,e. Two electrodes are connected to the device using wires for electrical measurements (Figure 3e). The same fabrication procedure is applied to all the other LCD layers. In total, five sets of TENG devices were fabricated for this study, designated as LCDW1-TENGs to LCDW5-TENGs, corresponding to each LCD layer used. The performance of the LCD-TENG devices was evaluated in vertical contact-separation mode with a hand-tapping force of ≈7 N at a frequency of 3–4 Hz at room temperature and a relative humidity of 45% RH. Electrical output measurements, including open-circuit voltage (V_{oc}) and short-circuit current (I_{sc}), were recorded using a digital storage oscilloscope (Tektronix TBS-1102) and a low-noise current preamplifier (SR570, Stanford Research

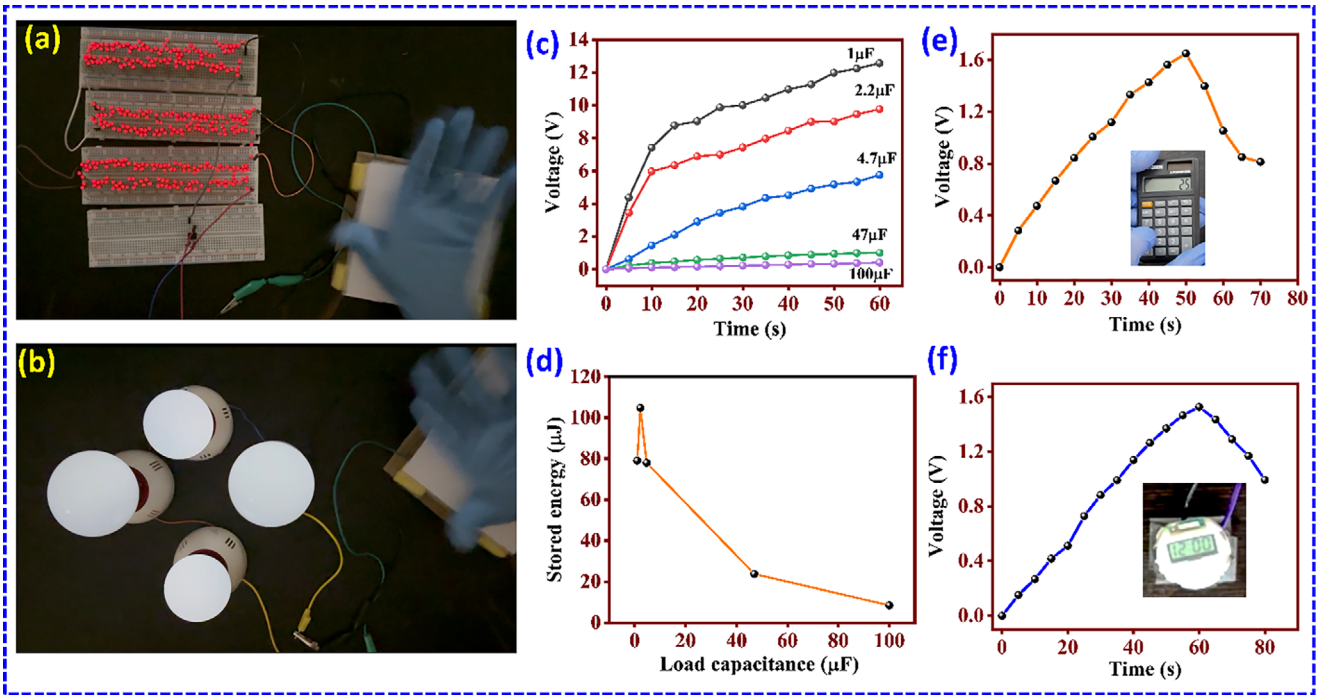

Figure 7. a) Photographs of the ON condition of the 360 LEDs, b) Four LED lamps powered by TENG, c) charging profiles of the various capacitors by the TENG, d) Energy stored by the capacitors, capacitor charging and discharging profiles while powering e) calculator, and f) digital watch.

Systems). The stability of the TENG devices was tested over 6000 cycles using machine tapping.

3. Results and Discussion

Figure 4a–e shows the responses of the fabricated LCD-TENG devices featuring various opposing friction layers for each fixed LCD layer. All the TENG devices exhibited similar trend in output voltage and current. The highest output response was recorded for a fixed FEP layer combined with all other LCD layers, and a comparison of these responses is depicted in Figure 4f. Among all the layers, the TENG based on LCD layer 4 (LCDW4) displayed the highest V_{oc} of ≈470 V and I_{sc} of ≈ 143 μA, and it was selected for further studies.

The working principle of the LCDW4 TENG is based on the combined effects of triboelectricity and electrostatic induction, as illustrated in **Figure 5**. Operating in a vertical contact-separation mode, it efficiently converts external mechanical energy into electrical energy when subjected to an applied force. In its initial state, the frictional layers remain separated by spacers, resulting in no potential difference and no current flow. When an external force, such as a hand tap, is applied, the LCDW4 layer and FEP film come into full contact, leading to charge exchange due to differences in their electronegativity. As FEP is a well-known triboelectric-negative material, it readily accepts electrons, while LCDW4 acts as a triboelectric-positive material. It is evident that when LCDW4 is paired with triboelectric-positive materials (e.g., PMMA, Kapton), it produces a lower output voltage, whereas pairing with triboelectric-negative materials (e.g., silicone, PTFE) results in a higher output voltage.[23,58–60] Once the external force is removed, the frictional layers separate, creating a potential difference that drives a transient electron flow from the negatively charged FEP electrode to the positively charged LCDW4 electrode. When the layers are fully separated, the system reaches electrostatic equilibrium. As the external force reestablishes contact between the layers, this equilibrium is disrupted, and the electrostatic induction charge is transferred through an external load. This continuous process of contact and separation generates an alternating current in the external circuit.

Figure 6a,b depicts the responses of the LCDW4-FEP TENG device under a switching polarity test configuration during repeated hand tapping. This test confirms that the observed electrical output originates from the TENG device itself and is not influenced by any external noise or spurious signals. Additionally, the load characteristics of the LCDW4-FEP TENG were studied by varying the load resistance up to 100 MΩ, as presented in Figure 6c. The results indicate that the output voltage increases with rising load resistance, eventually saturating at higher resistance levels, resembling open-circuit behavior. Conversely, the current decreases with increasing load resistance due to ohmic losses. The instantaneous power density of the LCDW4-FEP TENG was calculated based on the load characteristic data, revealing a maximum power density of 5.04 W m^{-2} at a load resistance of 1 MΩ, as shown in Figure 6d. Furthermore, the power density of the other LCDW TENG (1-5) devices were also evaluated and are presented in Figure S2 (Supporting Information). The LCDW4-FEP TENG device exhibited the highest power density among all the tested devices.

The long-term stability of the LCDW4-FEP TENG was assessed in a test comprising 20 min of machine tapping at a frequency of 5–6 Hz, amounting to ≈ 6000 cycles, and consistent output responses were recorded, as shown in Figure 6e. The change in

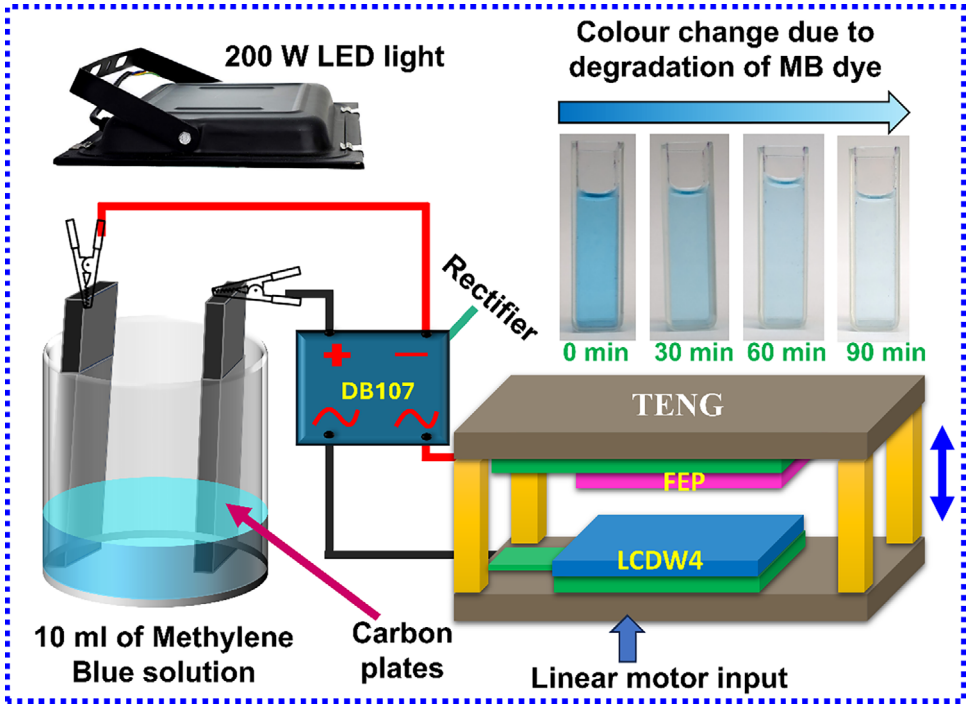

Figure 8. Schematics of the TENG assisted photocatalytic setup to degrade MB organic dye.

the output voltage was due to the variation in the force applied by the tapping machine. No evidence of surface degradation or cracks was observed on the frictional layer after the stability test.

The AC output of the TENG was rectified using DB 107 IC and the resulting DC output (pulsed) was utilized for different applications. The DC output of the TENG was used to briefly power a series of 360 red LEDs and four LED lamps with each hand tap, as shown in real-time videos (Videos S1 and S2, Supporting Information). **Figure** 7a,b displays photographs of the glowing LEDs and LED lamps powered by the TENG. Additionally, the TENG

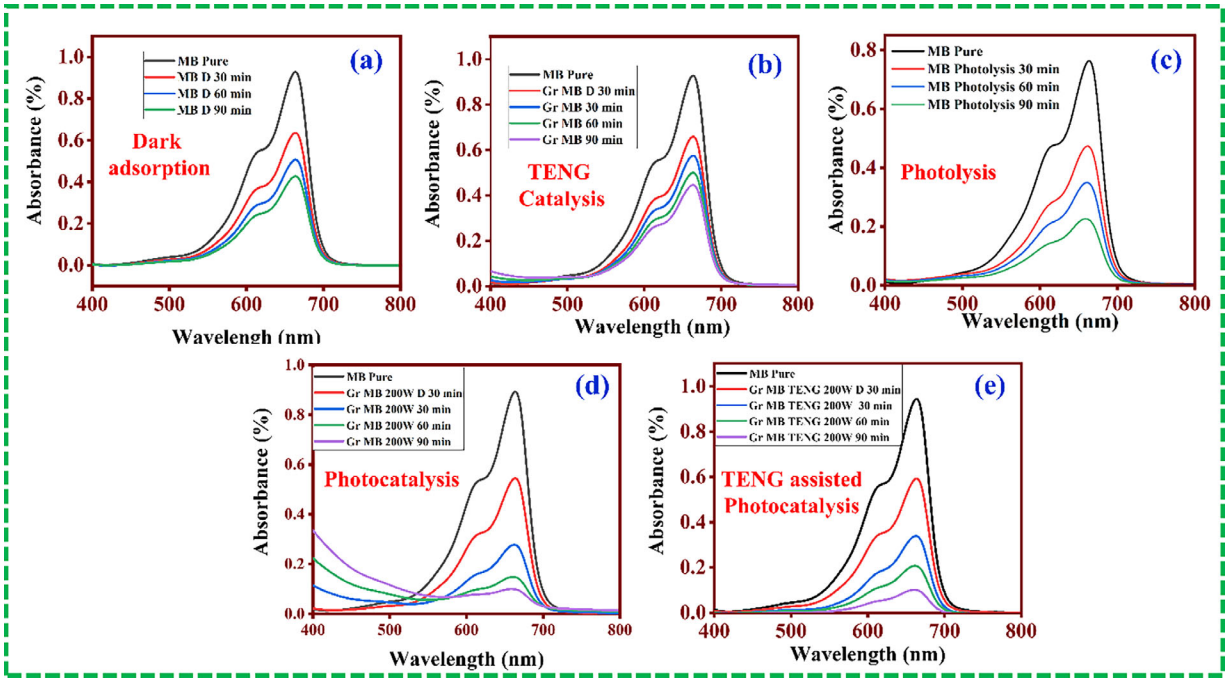

Figure 9. a) Absorbance spectra of dark adsorption, b) TENG only catalytic reactions, c) photolysis, d) photocatalysis, and e) TENG assisted photocatalysis of MB dye pollutant.

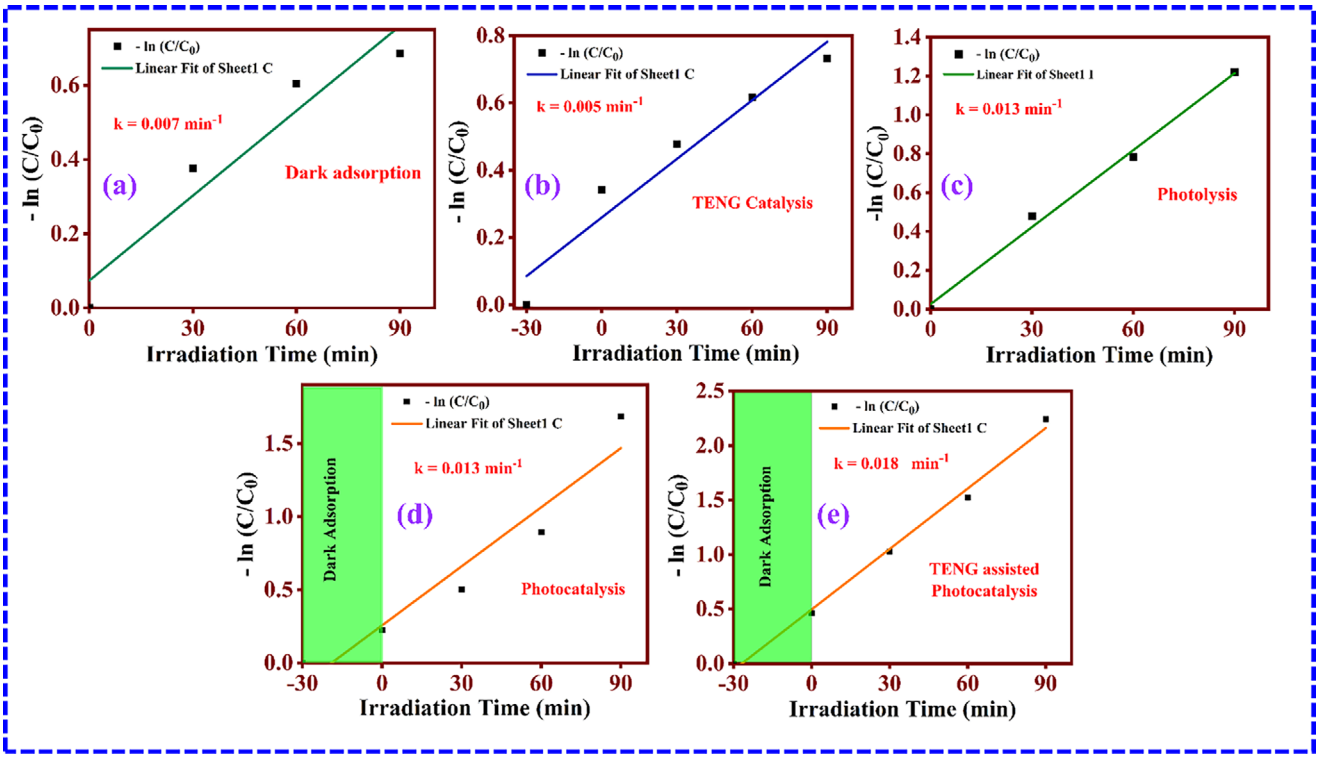

Figure 10. a) Pseudo-first order rate constants of dark adsorption, b) TENG only catalytic reactions, c) photolysis, d) photocatalysis, e) and TENG assisted photocatalysis for MB dye.

DC output was used to charge various capacitors, enabling the operation of the electronic devices. Figure 7c presents the charging curves of different capacitors over 60 s under continuous hand tapping, while Figure 7d illustrates the maximum energy stored in these capacitors. Furthermore, the TENG was successfully applied to power electronic devices such as a calculator and a digital watch through a power management circuit (Videos S3 and S4, Supporting Information). Initially, a 47 μF capacitor was charged to 1.6 V in 52 s and subsequently used to power a calculator for ≈ 14 s continuously (Figure 7e). Similarly, another 47 μF capacitor was charged to 1.52 V in 60 s and later it was used to power a digital watch for 14 s (Figure 7f). This demonstration underscores the potential of TENG technology for developing self-powered electronic devices in the future using the discarded LCD component layers.

4. TENG Assisted Photocatalytic Degradation

Photocatalytic degradation was performed for the graphite electrode material powered by a TENG device to demonstrate the degradation of organic contaminants under visible light irradiation using a 200 W LED light. MB dye was chosen as the target pollutant for demonstrating degradation. The photograph of the TENG assisted catalytic degradation experimental set up is provided in the Figure S3 (Supporting Information). The MB dye was dissolved in deionized water to achieve a solution concentration of 5 mg L^{-1} and a pH of 6. High-quality glassy carbon plate electrodes were utilized as the photocatalyst to degrade 10 mL of the contaminant solution. The MB dye and electrodes were placed in a 25 mL borosilicate beaker located 10 cm from the LED light (**Figure 8**). The two graphite electrodes were positioned vertically without touching each other, with an immersion area of ≈4 cm^2 inside the reaction container. The pair of carbon plates immersed in the reaction container (serving as cathode and anode) were connected to the DC output of the linear motor-driven TENG device. The Linear motor is run to operate the TENG for 15 min to generate electricity, followed by a 5-min interval to minimize the heating effect. The absorption spectrum of the initial and degrading MB dye solutions in the presence of the carbon plates catalyst was measured every 30 min for a total of 90 min using a UV-Visible spectrometer (Analytik Jena, SPECORD 210 PLUS).

The schematics of the TENG-assisted photocatalytic system for the degradation of MB dye is depicted in Figure 8. To demonstrate the enhanced pollutant degradation performance of the TENG device, the catalytic reactions were performed in five different types. The catalytic reactions carried out in the absence of light include dark adsorption and TENG-assisted catalytic reactions. Subsequently, the reactions conducted in the presence of light are categorized as photolysis, photocatalysis, and TENG-assisted photocatalysis.

The characteristic absorbance of the MB solution at 664 nm varied through multiple approaches (Dark, TENG, photolysis, photocatalysis, and TENG-assisted photocatalysis) over different reaction periods, as shown in **Figure 9a–e**. The dark adsorption is conducted for 30 min to achieve saturation (referred to as D 30 min) before evaluating the catalytic activity of all possible reactions. The porous nature of the carbon plates significantly

Table 1. Comparison of degradation kinetic parameters of all the set of catalytic reactions.

Type of Reaction	Rate constant [k] min^{-1}	Degradation efficiency [η] %
Dark Adsorption	0.007	49.7
TENG only catalytic reaction	0.005	51.9
Photolysis	0.013	70.5
Photocatalysis	0.013	81.4
TENG assisted Photocatalysis	0.018	89.4

reduces the pollutant concentration through dark adsorption. The equation provided below expresses the kinetics of degradation under various experimental conditions:

$$-\ln\left(C/C_0\right) = kt \quad (1)$$

C_0, C, and k represent the initial equilibrium concentration, actual dye concentration at reaction time t, and rate constants, respectively. The plot between irradiation time (t) versus -ln (C/C_0) follows the pseudo-first-order kinetics for all the set of reactions as shown in **Figure 10**. The slope of the curve, which is described as the rate constant k, is estimated to be 0.01 min^{-1} for photocatalysis and TENG-assisted photocatalysis. This indicates that the presence of a catalyst under light irradiation significantly increases the rate of reaction. The degradation kinetic parameters of all the catalytic reactions are summarized in **Table 1**.

The initial and final solution concentrations were measured to assess the degradation efficiency (η) of MB dye for photolysis and photocatalysis, as illustrated in **Figure 11**. The results suggest that TENG-assisted photocatalysis significantly outperforms other catalytic reactions in terms of pollutant degradation due to enhanced photoelectron cooperation. The TENG-only catalytic reaction, with an η value of 51.9% (≈2% higher than dark adsorption), indicates that the electrode material is viable as a source to power the electrocatalytic process even in the absence of light irradiation, rather than solely as a TENG-assisted electro-photocatalysis. Increase in degradation efficiency for TENG-assisted photocatalysis (89.4%) compared to photocatalysis (81.9%) demonstrates the significant contribution of TENG to the system. TENG promotes the separation and migration of photogenerated electron-hole pairs in photocatalysts which diminishes the recombination rate of these charge carriers, a crucial constraint in conventional photocatalysis, thus considerably enhancing the photocatalytic efficiency.[56] TENG's electric field and current promote the formation of reactive species such as hydroxyl radicals (^{-}OH), superoxide radicals ($^{-}O_2^{\bullet}$), and hydrogen peroxide (H_2O_2). These species are extremely competent in degrading organic pollutants and harmful gases.[61] The increased reactive oxygen species generation leads to faster and more complete disintegration of pollutants compared to photocatalysis alone. The probable mechanism for the TENG assited photocatalysis is represented in Figure 11f involving the ionization and migration of molecules and charge carriers to the respective electrodes. Furthermore, TENG (AC) assisted photocatalytic experiment was carried out without rectification of the output and a degradation efficiency of 71.5% is only obtained and the results are presented in Figure S4 (Supporting Information). The alternating flow of electron flow can drive certain

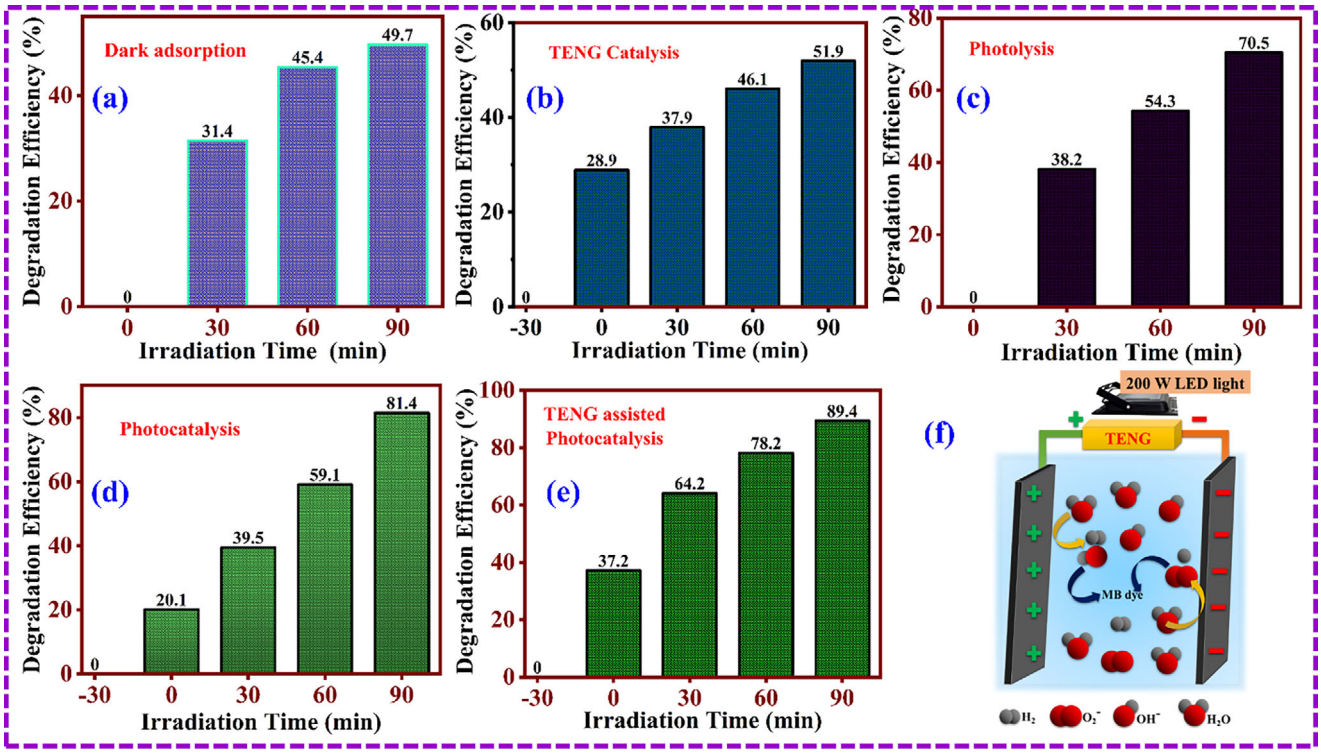

Figure 11. a) Degradation efficiency (η) of the dark adsorption, b) TENG only catalytic reactions, c) photolysis, d) photocatalysis, and e) TENG assisted photocatalysis f) Plausible mechanism of TENG assisted photodegradation of MB dye pollutant.

electrochemical reactions in the photocatalytic setup which in turn hamper the electrocatalytic processes thus reduced efficiency. To remain compatible with electrocatalytic systems, a TENG system requires unidirectional electron flow (DC output) which can be achieved through circuit rectification. The steady flow of electrons in one direction contribute to drive redox processes efficiently.[57,62] The continuous current output induces more stable and regulated reaction conditions, boosting charge usage and overall catalytic efficiency.[63] Hence, DC output from the TENG system provides improved charge separation, reduced recombination, faster formation of reactive species offering a higher catalytic efficiency. However, it is important to consider the choice of the catalytic electrode and the relatively small immersed area of the carbon plate, which limits the charge transfer mechanism within the reaction container. The incident photon flux significantly impacts the utilization of photoinduced charge carriers from the photocatalyst. Nevertheless, the TENG-driven photocatalytic setup under illumination with cost-effective LED light shows moderate increase in efficiency in degrading the MB dye pollutant. However, the TENG assisted photocatalytic degradation is promising and may create opportunities to develop suitable photocatalysts in various dimensions to maximize the area in the reaction container, facilitating effective charge transfer through TENG-generated rectified DC electricity while optimizing the use of light irradiation.

5. Conclusion

The present study investigates the upcycling of e-waste generated from discarded LCD displays for the fabrication of TENGs and their applications in self-powered electronics and wastewater treatment. The LCD waste-based TENG produced an output power density of 5.04 W m^{-2} with FEP as the opposite frictional layer. The LCDW4-FEP TENG can power up to 360 red LEDs and four LED lamps momentarily for each tap, and it is also demonstrated to power portable electronic devices for a few seconds. Beyond the regular application of TENGs, the LCDW4-FEP TENG was utilized for wastewater treatment through TENG-assisted photocatalysis. Results indicated that TENG-assisted photocatalysis improved significantly the degradation efficiency of MB dye. The coupled activity of the TENG and light promotes faster charge generation, minimizes recombination and reduces time consumption thereby increasing the overall efficiency. These findings pave the way for integrating e-waste into energy-harvesting devices for self-powered devices and dye pollutant treatment, supporting the circular economy concept. Future research can focus on scaling these WTE devices to larger sizes and exploring new e-waste components for TENG-based clean energy generation systems.

Supporting Information

Supporting Information is available from the Wiley Online Library or from the author.

Acknowledgements

The authors R.R.K., D.P.J., and K.U.K. thank the Director of the National Institute of Technology-Warangal for his constant encouragement and infrastructure support.

Conflict of Interest

The authors declare no conflict of interest.

Author Contributions

A.K. performed data curation, investigation, methodology, formal analysis, validation, visualization, wrote original draft, G.M. performed data curation, investigation, methodology, wrote, reviewed, and edited, N.M. performed methodology, formal analysis, project administration, resources, software, wrote, reviewed, and edited, V.M. performed data curation, formal analysis, resources, K.U.K. performed formal analysis, resources, visualization, wrote, reviewed, and edited, P.J.D. performed supervision, methodology, validation, wrote original draft; wrote, reviewed, and edited, R.R.K. performed conceptualization, project administration, supervision, methodology, validation, visualization, wrote original draft; wrote, reviewed, and edited.

Data Availability Statement

The data that support the findings of this study are available from the corresponding author upon reasonable request.

Keywords

Energy harvesting, e-waste, organic pollutant degradation, triboelectric nanogenerators, waste-to-energy

Received: February 27, 2025
Revised: June 3, 2025
Published online: June 23, 2025

[1] S. Kaza, L. Yao, P. Bhada-Tata, F. Van Woerden, *What a Waste 2.0: A Global Snapshot of Solid Waste Management to 2050*, The World Bank, Washington, DC **2018**.
[2] D. M.-C. Chen, B. L. Bodirsky, T. Krueger, A. Mishra, A. Popp, *Environ. Res. Lett.* **2020**, *15*, 074021.
[3] A. Kumar, A. K. Thakur, G. K. Gaurav, J. J. Klemeš, V. K. Sandhwar, K. K. Pant, R. Kumar, *Environ. Sci. Pollut. Res.* **2023**, *30*, 105030.
[4] A. Maalouf, A. Mavropoulos, *Waste Manage. Res.* **2023**, *41*, 936.
[5] W. Foster, U. Azimov, P. Gauthier-Maradei, L. C. Molano, M. Combrinck, J. Munoz, J. J. Esteves, L. Patino, *Renew. Sustain. Energy Rev.* **2021**, *135*, 110226.
[6] H. Madkhali, S. Duraib, L. Nguyen, M. Prasad, M. Sharma, S. Joshi, *Knowledge* **2023**, *3*, 163.
[7] S. D. Anuar Sharuddin, F. Abnisa, W. M. A. Wan Daud, M. K. Aroua, *Energy Convers Manag.* **2016**, *115*, 308.
[8] S. Yoon, J. Lee, *Energy* **2024**, *289*, 130029.
[9] M. F. M. A. Zamri, S. Hasmady, A. Akhiar, F. Ideris, A. H. Shamsuddin, M. Mofijur, I. M. R. Fattah, T. M. I. Mahlia, *Renew. Sustain. Energy Rev.* **2021**, *137*, 110637.
[10] L. Makarichi, W. Jutidamrongphan, K. anan Techato, *Renew. Sustain. Energy Rev.* **2018**, *91*, 812.
[11] H. Zhou, S. Sun, Y. Xu, Y. Zhang, S. Yi, C. Wu, *j. Energy Chem.* **2024**, *96*, 611.
[12] X. Peng, Y. Jiang, Z. Chen, A. I. Osman, M. Farghali, D. W. Rooney, P.-S. Yap, *Environ. Chem. Lett.* **2023**, *21*, 765.
[13] K. U. Kumar, S. Hajra, G. Mohana Rani, S. Panda, R. Umapathi, S. Venkateswarlu, H. J. Kim, Y. K. Mishra, R. R. Kumar, *Adv. Compos. Hybrid Mater.* **2024**, *7*, 91.

[14] S. A. Basith, G. Khandelwal, D. M. Mulvihill, A. Chandrasekhar, *Adv. Funct. Mater.* **2024**, *34*, 2408708.
[15] A. A. Ahmed, T. F. Qahtan, T. O. Owolabi, A. O. Agunloye, M. Rashid, M. S. Mohamed Ali, *J. Clean Prod.* **2024**, *448*, 141354.
[16] F. R. Fan, Z. Q. Tian, Z. L. Wang, *Nano Energy* **2012**, *1*, 328.
[17] C. Wu, A. C. Wang, W. Ding, H. Guo, Z. L. Wang, *Adv. Energy Mater.* **2019**, *9*, 1802906.
[18] G. Zhu, B. Peng, J. Chen, Q. Jing, Z. L. Wang, *Nano Energy* **2014**, *14*, 126.
[19] D. Choi, Y. Lee, Z. H. Lin, S. Cho, M. Kim, C. K. Ao, S. Soh, C. Sohn, C. K. Jeong, J. Lee, M. Lee, S. Lee, J. Ryu, P. Parashar, Y. Cho, J. Ahn, I. D. Kim, F. Jiang, P. S. Lee, G. Khandelwal, S. J. Kim, H. S. Kim, H. C. Song, M. Kim, J. Nah, W. Kim, H. G. Menge, Y. T. Park, W. Xu, J. Hao, et al., *ACS Nano* **2023**, *17*, 11087.
[20] J. Zhao, J. Mo, B. Luo, C. Cai, Y. Liu, G. Du, Y. Shao, X. Meng, Z. Wei, S. Nie, *Device* **2025**, *3*, 100557.
[21] C. Cai, B. Luo, Y. Liu, Q. Fu, T. Liu, S. Wang, S. Nie, *Mater. Today* **2022**, *52*, 299.
[22] R. Zhang, H. Olin, *EcoMat* **2020**, *2*, e12062.
[23] J. Wang, Y. Chen, Y. Xu, J. Mu, J. Li, S. Nie, S. Chen, F. Xu, *Sustain. Energy Fuels* **2022**, *6*, 1974.
[24] P. Lu, Y. Yang, B. Luo, C. Cai, T. Liu, S. Zhang, M. Chi, T. Zhao, J. Wang, X. Meng, Y. Bai, Y. Shao, G. Du, S. Wang, S. Nie, *Adv. Funct. Mater.* **2025**, *35*, 2418336.
[25] C. Cai, T. Liu, X. Meng, B. Luo, M. Chi, J. Wang, Y. Liu, S. Zhang, C. Gao, Y. Bai, S. Wang, S. Nie, *ACS Nano* **2025**, *19*, 396.
[26] T. Liu, Z. Zhao, R. Liang, H. He, Y. Liu, K. Yu, M. Chi, B. Luo, J. Wang, S. Zhang, C. Cai, S. Wang, S. Nie, *Adv. Funct. Mater.* **2025**, 2500207.
[27] S. R. Begum, A. Chandrasekhar, *ACS Appl. Electron. Mater.* **2023**, *5*, 1347.
[28] S. Potu, A. Kulandaivel, B. Gollapelli, U. K. Khanapuram, R. K. Rajaboina, *Mater. Sci. Eng.: R: Rep.* **2024**, *161*, 100866.
[29] M. Shanbedi, H. Ardebili, A. Karim, *Prog. Polym. Sci.* **2023**, *144*, 101723.
[30] R. K. Rajaboina, U. K. Khanapuram, A. Kulandaivel, *Adv. Sens. Res.* **2024**, *3*, 2400045.
[31] M. Zhang, H. Du, K. Liu, S. Nie, T. Xu, X. Zhang, C. Si, *Adv. Compos. Hybrid Mater.* **2021**, *4*, 865.
[32] G. Khandelwal, A. Chandrasekhar, N. R. Alluri, V. Vivekananthan, N. P. Maria Joseph Raj, S. J. Kim, *Appl. Energy* **2018**, *219*, 338.
[33] B. Zhang, L. He, J. Wang, Y. Liu, X. Xue, S. He, C. Zhang, Z. Zhao, L. Zhou, J. Wang, Z. L. Wang, *Energy Environ. Sci.* **2023**, *16*, 3873.
[34] C. S. Patil, Q. M. Saqib, S. R. Patil, M. Noman, M. Y. Chougale, R. A. Shaukat, J. Kim, Y. Ko, T. D. Dongale, J. Bae, *Nano Energy* **2024**, *121*, 109205.
[35] M. U. Bukhari, A. Khan, K. Q. Maqbool, A. Arshad, K. Riaz, A. Bermak, *Energy Rep.* **2022**, *8*, 1687.
[36] R. F. S. M. Ahmed, S. Amini, S. M. Ankanathappa, K. Sannathammegowda, *Waste Manage.* **2024**, *178*, 1.
[37] V. L. Suneetha, V. Mahesh, P. Supraja, M. Navaneeth, K. U. Kumar, R. R. Kumar, *Energy Technol.* **2025**, 13.
[38] S. Natarajan, K. Krishnamoorthy, A. Sathyaseelan, V. K. Mariappan, P. Pazhamalai, S. Manoharan, S. J. Kim, *Nano Energy* **2022**, *101*, 107595.
[39] E. Zhao, K. Jiang, B. Li, X. Liu, F. Zeng, L. Chen, H. Zhang, Z. Zhu, *Nanotechnology* **2022**, *33*, 495401.
[40] W.-G. Kim, D.-W. Kim, I.-W. Tcho, J.-K. Kim, M.-S. Kim, Y.-K. Choi, *ACS Nano* **2021**, *15*, 258.
[41] X. Cao, Y. Xiong, J. Sun, X. Xie, Q. Sun, Z. L. Wang, *Nanomicro Lett.* **2023**, *15*, 14.
[42] J. Wang, Y. Liu, Z. Wei, T. Liu, Y. Li, B. He, B. Luo, C. Cai, S. Zhang, M. Chi, C. Shi, S. Wang, S. Nie, *Adv. Funct. Mater.* **2025**, *35*, 2424185.
[43] Y. Liu, J. Wang, T. Liu, Z. Wei, B. Luo, M. Chi, S. Zhang, C. Cai, C. Gao, T. Zhao, S. Wang, S. Nie, *Nat. Commun.* **2025**, *16*, 383.
[44] M. Navaneeth, S. Potu, A. Babu, B. Lakshakoti, R. K. Rajaboina, U. Kumar K, H. Divi, P. Kodali, K. Balaji, *ACS Sustain. Chem. Eng.* **2023**, *11*, 12145.
[45] Z. Li, J. Chen, H. Guo, X. Fan, Z. Wen, M. H. Yeh, C. Yu, X. Cao, Z. L. Wang, *Adv. Mater.* **2016**, *28*, 2983.
[46] F. Dong, Z. Pang, S. Yang, Q. Lin, S. Song, C. Li, X. Ma, S. Nie, *ACS Nano* **2022**, *16*, 3449.
[47] X. Liu, J. Mo, W. Wu, H. Song, S. Nie, *Appl. Catal. B* **2022**, *312*, 121422.
[48] S. Shen, J. Fu, J. Yi, L. Ma, F. Sheng, C. Li, T. Wang, C. Ning, H. Wang, K. Dong, Z. L. Wang, *Nanomicro Lett.* **2021**, *13*, 194.
[49] T. Lu, Y. Zhang, Z. Wang, S. Li, L. Zheng, H. Li, *Nano Energy* **2024**, *127*, 109712.
[50] S. Chen, N. Wang, L. Ma, T. Li, M. Willander, Y. Jie, X. Cao, Z. L. Wang, *Adv. Energy Mater.* **2016**, *6*, 1501778.
[51] S. B. Jeon, S. Kim, S. J. Park, M. L. Seol, D. Kim, Y. K. Chang, Y. K. Choi, *Nano Energy* **2016**, *28*, 288.
[52] W. Qu, C. Zhong, P. Luan, W. Shi, L. Geng, G. Shi, R. Chen, *Front. Energy Res.* **2024**, *12*, 1324866.
[53] C. Tortajada, *NPJ Clean Water* **2020**, *3*, 22.
[54] O. Ejiohuo, H. Onyeaka, A. Akinsemolu, O. F. Nwabor, K. F. Siyanbola, P. Tamasiga, Z. T. Al-Sharify, *Water Biol. Sec.* **2025**, *4*, 100341.
[55] W. Ahmad, R. D. Alharthy, M. Zubair, M. Ahmed, A. Hameed, S. Rafique, *Sci. Rep.* **2021**, *11*, 17006.
[56] M. M. Uddin, T. M. Dip, S. I. Tushar, A. Sayam, H. R. Anik, M. d. R. A. Arin, A. Talukder, S. Sharma, *ACS. Omega* **2025**, *10*, 26.
[57] F. Dong, Z. Pang, Q. Lin, D. Wang, X. Ma, S. Song, S. Nie, *Nano Energy* **2022**, *100*, 107515.
[58] Y. Liu, J. Mo, Q. Fu, Y. Lu, N. Zhang, S. Wang, S. Nie, *Adv. Funct. Mater.* **2020**, *30*, 2004714.
[59] Y. J. Kim, J. Lee, S. Park, C. Park, C. Park, H. J. Choi, *RSC. Adv.* **2017**, *7*, 49368.
[60] H. Zou, L. Guo, H. Xue, Y. Zhang, X. Shen, X. Liu, P. Wang, X. He, G. Dai, P. Jiang, H. Zheng, B. Zhang, C. Xu, Z. L. Wang, *Nat. Commun.* **2020**, *11*, 2093.
[61] X. Hao, T. Huang, M. Li, Y. Pan, L. Liao, K. Zhang, A. Qin, *J. Mater. Chem. A Mater.* **2023**, *11*, 16403.
[62] S. Gao, Y. Chen, J. Su, M. Wang, X. Wei, T. Jiang, Z. L. Wang, *ACS Nano* **2017**, *11*, 3965.
[63] Y. Gao, L. He, D. Liu, J. Zhang, L. Zhou, Z. L. Wang, J. Wang, *Nat. Commun.* **2024**, *15*, 4167.